Robotica (2008) volume 26, pp. 219–227. © 2007 Cambridge University Press
doi:10.1017/S0263574707003797 Printed in the United Kingdom

Stabilization and equilibrium control of a new pneumatic cart-seesaw system

J. Lin,* J. H. Zhan and Julian Chang

Department of Mechanical Engineering, Ching Yun University, Jung-Li City, Taiwan 320, R.O.C.

(Received in Final Form: July 22, 2007. First published online: August 30, 2007)

SUMMARY

This investigation describes the mechanical configuration and control environment for a novel cart-seesaw system. This mechanism is called a super articulated mechanical system (SAMS). The system comprises a cart that slides on the pneumatic rodless cylinder. The rodless cylinder is double-acting with the carrier bracket, on which a cart is a pinion mechanism for the tracks. The cart-seesaw system brings the cart from any initial position to a desired position on the seesaw by applying an appropriate force to the cart and thus adjusting the angle of the seesaw. The position of a cart denotes the first degree of freedom, which is activated by a pneumatic proportional valve, and the angle of the seesaw indicates the second degree of freedom that is not actuated. Consequently, the proposed new pneumatic cart-seesaw system is straightforward to construct and direct to operate in different scenarios of performance. A state feedback controller is applied for stabilization of the equilibrium point of the system. Moreover, this study adds a supervisory controller that takes control action in extreme situations. Test results reveal excellent properties in control performance. The proposed product can be extensively applied in SAMS and pneumatic control for robotics control laboratory.

KEYWORDS: Robots; Ball-and-beam; Cart-seesaw system.

1. Introduction

Underactuated mechanisms have recently attracted significant attention, owing to their ability not only to represent a rich class of control system from a control stand point but also to reduce the cost of robots by decreasing the link mass and the number of robot actuators.[1] In contrast to the system with full controls, a super articulated mechanical system (SAMS) is a controlled underactuated mechanical system in which the dimension of the configuration space exceeds the dimension of the control input space. For example, inverted pendulum on a cart, ball and beam problem, mass sliding on a cart and robots with joint elasticity, underactuated bipedal robot, nonholonomic mobile robot, etc., all is SAMS.[2]

A super-articulated mechanical system presents challenges that are not found in a system with full controls, in which the dimensions of the configuration space equals the dimension of the control input space. For instance, controllability is not easy to determine locally in an SAMS, since it is generally implied in a system with full control. Control synthesis is also more complex in an SAMS than in a system with full control.[3] Literature[4–6] on motion planning and control of nonholonomic systems has indicated the difficult yet interesting features of control synthesis for SAMS.

Control design for underactuated bipedal robot is a fascinating topic in robotics.[7,8] A planar underactuated bipedal robot with an impulsive foot model is considered in ref. [7]. A feedback design method is proposed that integrates actuation in the single and double support phases. Nevertheless, this paper presents a simple feedback control design with no supervisory control to take control action in extreme situations. Similarly, the robust control of underactuated bipeds using sliding modes is demonstrated in ref. [8]. A sliding mode control law has been developed for the biped to follow a human-like gait trajectory while keeping the torso nearly upright. The control law is too complicated to understand for the undergraduate students. Moreover, it lacks experimental implementation to verify the control algorithms.

The ball-and-beam system is a common undergraduate control laboratory experiment.[9] Control of the ball-and-beam system has been widely discussed in teaching and research literature—many classical control solutions can be found on the Internet and in introductory control textbooks. However, discovering a control law to stabilize the system remains an active topic of research discussion.

The ball-and-beam mechanism generally comprises a beam with a ball on it. The ball rolls on the beam according to the changing angle of the beam. A ball moving on a beam is a typical nonlinear dynamic system, which is often adapted to proof-test diverse control methods.[10] Such a system may be adopted as a control-training tool by engineering students to test industrial processes and their applications.

Moreover, the "ball and the beam" system is well documented as an example of a system that requires an active control system to maintain the ball at a desired beam position. Several approaches have been presented to control the ball-and-beam system during the past decades, for example, input–output feedback linearization,[10] robust nonlinear control,[11,12] and fuzzy logic control.[13–15] However, all of the above papers are based on the same conventional ball-on-beam plant, in which the ball is rolling on the beam according to the changing angle of the beam. The system lacks a new mechanism for other control purposes.

Pneumatic cylinders are sometimes considered to offer a better alternative to electrical or hydraulic actuators for

* Corresponding author. E-mail: jlin@cyu.edu.tw

certain types of applications. The pneumatic cylinder is being widely employed as an important driving element in industrial applications due to its simple, cheap, and excellent performance. The development of control technology increases the requirement for control precision. Pneumatic actuators are often adopted in applications requiring high power-to-weight ratio, combined with low price and clean operation. They are also suitable for clean environments, and are safe and easier to use. Unfortunately, owing to the compressibility of air, highly nonlinear behavior, and time delay resulting from the slow propagation of pressure waves, position and force control of these actuators are difficult.[16] Researchers have tried controlling the pneumatic actuators using different approaches, including adaptive control[17,18] and sliding mode control,[19–22] during the past decade. However, controlling the position and force of these actuators in applications that require high bandwidth is difficult. This is mainly due to the compressibility of air and highly nonlinear flow through pneumatic system components.

The review of the above papers indicates that no researchers have attempted to control a ball-and-beam mechanism by a pneumatic cylinder for actuation. Hence, the main goal of this research is to develop a new ball-and-beam mechanism for laboratory exercises and student projects in subjects covering robot control. This new mechanism is defined as a cart-seesaw system. The experimental implementation is setup to verify the proposed control methodology. The seesaw can rotate only in a vertical plane with one degree of freedom, and the cart slides along the seesaw by applying a force with a pneumatic device. The objective of this experiment is to achieve a desired sliding mass position on the cart. This study investigation serves as a reference of the achievable control behavior for the underactuated mechanism, and covers the extension of the curriculum to the control of the underactuated robots. Finally, the proposed product in this paper can be extensively applied in SAMS and pneumatic control for a robotics control laboratory.

2. System Configuration

2.1. System description

The ball-and-beam mechanism consists of a beam and a ball on it. The ball rolls on the beam according to the changing angle of the beam. The proposed ball-and-beam-like mechanism replaces the ball is replaced with a cart, which slides "frictionlessly" on the pneumatic rodless cylinder. The proposed cart-seesaw system consists of one sliding cart, which is coupled via rack and pinion mechanism to tracks mounted on a seesaw. Forces are applied to the cart via pneumatic actuator. The seesaw is joined and frees to rotate in unison about the pivot point. Figure 1 illustrates the conceptual model of a pneumatic cart-seesaw system.

Pneumatic servos have been less widely analyzed than hydraulic servos, particularly because the equations for compressible flow are more difficult than for the incompressible flow to handle. The difference in performance arises because pneumatic servos use a very compressible fluid. For example, air is introduced into a cylinder when the valve is opened, and sufficient gas must then flow into the cylinder volume to raise the pressure and build up sufficient force to overcome any spring preload or static friction. In hydraulic systems, a very small valve displacement causes pressure in the cylinder to rise immediately. Hence, a hydraulic system has a rapid initial response, while a pneumatic system exhibits a time delay. Since the fluid is compressible, the servo lacks stiffness, especially to external load disturbances. To achieve the stiff characteristics of hydraulics, these systems must either be large enough to absorb any load variation with a small change in pressure, or be provided with a large servo-valve that is capable of rapidly adding or removing gas.[23] However, the difficulty of the pneumatic system is not a main issue in this paper. Future work will address the difficulty problem of pneumatic systems.

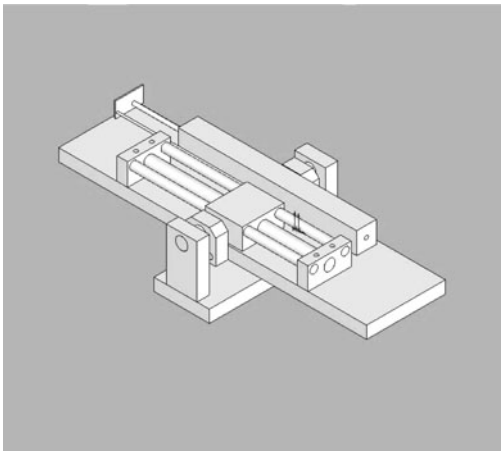

Fig. 1. Conceptual model of a pneumatic cart-seesaw system.

The experimental pneumatic system was composed of a pneumatic rodless cylinder 240 mm long, two controlled proportional valves, a measurement system comprising of two sensors (rotary potentiometer and linear potentiometer), a personal computer (PC), and a source of compressed air. The cylinder was double-acting, and had a carrier bracket on which a sliding cart was attached to the tracks by a pinion mechanism. The air supply to the cylinder was manipulated by an electro-pneumatic transducer that provided an air pressure proportional to the supply voltage. Each direction of motion was selected by appropriate actuation of the two 3/2-way electro-valves (model type: SMC VEF 3121-1), which converted the electrical signal to proportional airflow. Figure 2 displays the pneumatic circuit.

A linear potentiometer was utilized to measure the position of the sliding cart. Additionally, the cart position r was measured from the seesaw center, and was positive if the cart was on the right side of the seesaw. Similarly, the rotary potentiometer was adopted to measure the seesaw angle. The seesaw angle θ was positive if the seesaw rotated counterclockwise from horizon.

The proposed system applies two mechanical stabilization systems: static balance and dynamic equilibrium. Structural bias or loading unbalance disturbances prevent the system sensor from accurately measuring the equilibrium point. For instance, the seesaw angle should ideally be zero when the

https://doi.org/10.1017/S0263574707003797 Published online by Cambridge University Press

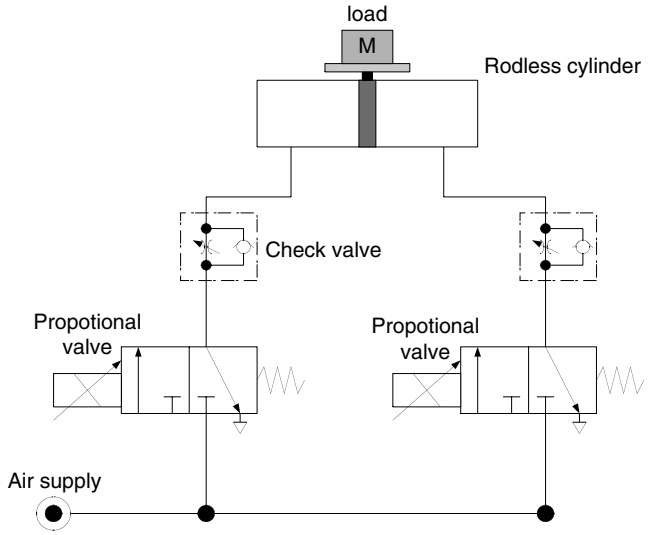

Fig. 2. Pneumatic circuit for cart-seesaw system.

cart moves to the center of the seesaw. This point is called the equilibrium point. However, due to the bias or loading unbalance disturbances existing in the original mechanism, the sensor for equilibrium point cannot accurately show the zero value. To solve this problem, an adjustable weight rod was installed as a counterbalance. This mechanism is called static balance apparatus. The counterweight modification method can guarantee that the seesaw angle equals zero when the cart position is located at the center of the seesaw. However, sensor system must adapt their sensing value during the experiment.

Furthermore, the seesaw falls to the definite direction instantaneously if the cart runs to a particular place, thus creating instantaneous dynamic instability. Hence, in dynamical improvement aspect, several torsion springs are installed underneath the seesaw to serve as a damping mechanism to absorb the impact and shock energy. Two torsion springs are installed underneath the seesaw in such a system. Figure 3 depicts the visualization of this cart-seesaw system, and indicates some important devices in such a system.

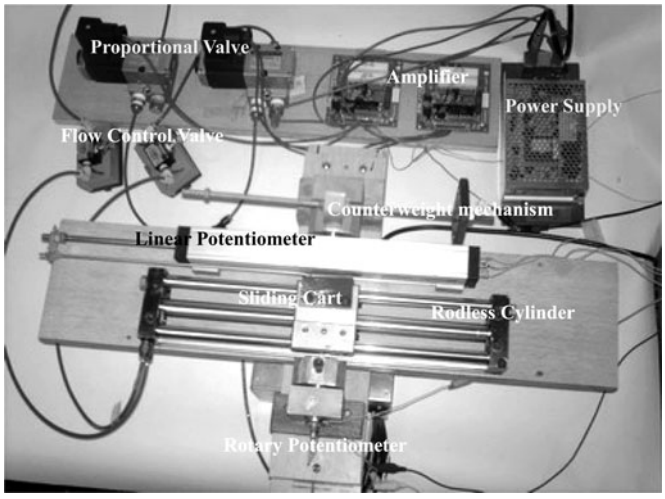

Fig. 3. Visualization of cart-seesaw system.

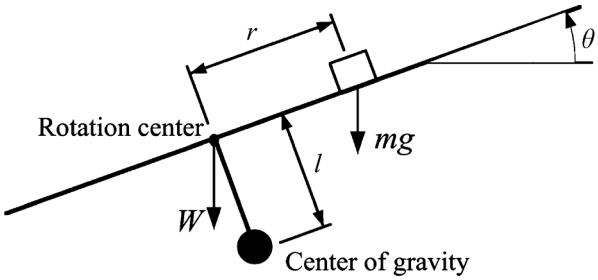

Fig. 4. Free-body diagram of the cart-seesaw system.

2.2. *Rotation center and center of gravity*

The designation of the rotation center determines the dynamic stability of the whole system. An inappropriately positioned rotation leads to an inherently unstable system. Hence, the overall cart-seesaw system can tilt while the cart is sliding. As revealed in Fig. 4, the distance of the rotation center to the center of gravity of the cart-seesaw system is l. The cart should move to the right as the seesaw rotates counterclockwise with angle θ to prevent the seesaw from tilting to the left. The distance between the cart and the rotation center is assumed to be r in this case. To prevent the cart-seesaw system from tilting, the moment of the clockwise side should be greater than that of the counterclockwise side. The resulting equation has the following form:

$$mg(r\cos\theta - l\sin\theta) > Wl\sin\theta \tag{1}$$

where W denotes the total weight of the seesaw, and m represents the sliding cart.

Therefore, Eq. (1) can be rewritten as

$$mgr\cos\theta > (mg\sin\theta + W\sin\theta)l. \tag{2}$$

Equation (2) demonstrates that a longer distance between the center of gravity and the rotation center l requires a larger value for r, i.e, the distance between the cart and the center of gravity. However, the mass of the sliding cart m is much smaller than the total weight of the seesaw W ($mg \ll W$). Therefore, the rotation center and the center of gravity are collocated on the same line in the proposed system, so that the distance between the center of gravity and the rotation center l is very small ($l \fallingdotseq 0$). This coincides with the requirement of Eq. (2), and can enhance the dynamic stability and prevent the cart-seesaw system from tilting. Hence, the mechanical configuration follows this concept to set up the system (Fig. 5).

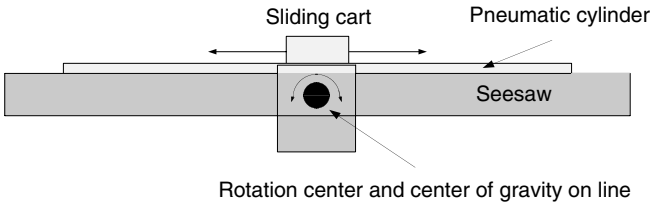

Fig. 5. Side view for the cart-seesaw system.

https://doi.org/10.1017/S0263574707003797 Published online by Cambridge University Press

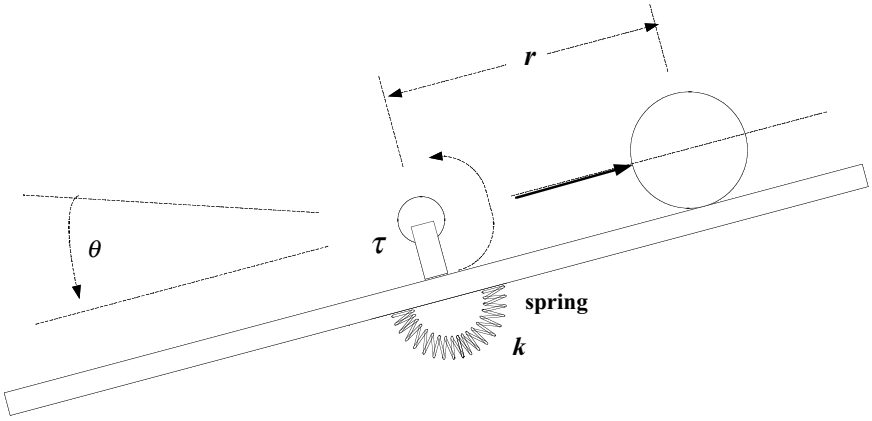

Fig. 6. Dynamic model for pneumatic cart-seesaw mechanism.

3. Dynamic Modeling

In this section, a mathematical model of the pneumatic cart-seesaw mechanism is obtained from independently known dynamics. Consider the cart-seesaw system illustrated in Fig. 6. The cart-seesaw system brings the cart from any initial position with any initial speed to a desired position on the seesaw by applying an appropriate force to the cart, and thus adjusting the angle of the seesaw. The cart sliding on the seesaw indicates the first degree of freedom, which is actuated by a pneumatic proportional control valve, and the angle of a seesaw represents the second degree of freedom, which is not actuated.

Let the moment of inertia of the seesaw be J, the mass of the sliding cart be M, and the gravity acceleration g. The torsion spring k is attached on the underneath of the seesaw to serve as the vibration damper in order to absorb the impact and shock energy. Selecting the beam angle θ and slide cart position r as generalized position coordinates for the system, using the Lagrangian formulation, the dynamic equations are given by

$$\begin{aligned} M\ddot{r} + Mg\sin\theta - Mr\dot{\theta}^2 &= \tau \\ (Mr^2 + J)\ddot{\theta} + 2Mr\dot{r}\dot{\theta} + Mgr\cos\theta + k\theta &= 0. \end{aligned} \tag{3}$$

The detailed derivation procedure of Eq. (3) is indicated as Appendix. Moreover, Eq. (3) can also be written in matrix form

$$\begin{bmatrix} M & 0 \\ 0 & Mr^2 + J \end{bmatrix}\begin{bmatrix} \ddot{r} \\ \ddot{\theta} \end{bmatrix} + \begin{bmatrix} 0 & -Mr\dot{\theta} \\ Mr\dot{\theta} & Mr\dot{r} \end{bmatrix}\begin{bmatrix} \dot{r} \\ \dot{\theta} \end{bmatrix} + \begin{bmatrix} 0 & 0 \\ 0 & k \end{bmatrix}\begin{bmatrix} r \\ \theta \end{bmatrix} + \begin{bmatrix} Mg\sin\theta \\ Mgr\cos\theta \end{bmatrix} = \begin{bmatrix} \tau \\ 0 \end{bmatrix}. \tag{4}$$

Compared with the robotic dynamics formulation, $\mathbf{M} = \left[\begin{smallmatrix} M & 0 \\ 0 & Mr^2+J \end{smallmatrix}\right]$ is the inertia matrix; $\mathbf{C} = \left[\begin{smallmatrix} 0 & -Mr\dot{\theta} \\ Mr\dot{\theta} & Mr\dot{r} \end{smallmatrix}\right]$ denotes the Coriolis/centripetal matrix; $\mathbf{K} = \left[\begin{smallmatrix} 0 & 0 \\ 0 & k \end{smallmatrix}\right]$ represents the stiffness matrix, and $\mathbf{G} = \left[\begin{smallmatrix} Mg\sin\theta \\ Mgr\cos\theta \end{smallmatrix}\right]$ is the gravity vector.

Furthermore,

$$\begin{aligned} \dot{\mathbf{M}} - 2\mathbf{C} &= \begin{bmatrix} 0 & 0 \\ 0 & 2Mr\dot{r} \end{bmatrix} - \begin{bmatrix} 0 & -2Mr\dot{\theta} \\ 2Mr\dot{\theta} & 2Mr\dot{r} \end{bmatrix} \\ &= \begin{bmatrix} 0 & 2Mr\dot{\theta} \\ -2Mr\dot{\theta} & 0 \end{bmatrix} \end{aligned}$$

indicates a skew-symmetric matrix.

By defining the state vector $x = [r \;\; \dot{r} \;\; \theta \;\; \dot{\theta}]^T = [x_1 \;\; x_2 \;\; x_3 \;\; x_4]^T$, the state space form is described as

$$\begin{aligned} \dot{x} &= \begin{bmatrix} \dot{x}_1 \\ \dot{x}_2 \\ \dot{x}_3 \\ \dot{x}_4 \end{bmatrix} = \begin{bmatrix} \dot{r} \\ \ddot{r} \\ \dot{\theta} \\ \ddot{\theta} \end{bmatrix} \\ &= \begin{bmatrix} x_2 \\ -g\sin x_3 + x_1 x_4^2 + (1/M)\tau \\ x_4 \\ -\dfrac{2Mx_1x_2x_4}{Mx_1^2 + J} - \dfrac{gx_1\cos x_3}{Mx_1^2 + J} - \dfrac{kx_3}{Mx_1^2 + J} \end{bmatrix} \\ &= f(x,\tau) = f(x) + g(x)\tau \end{aligned} \tag{5}$$

where

$$f(x) = \begin{bmatrix} x_2 \\ -g\sin x_3 + x_1 x_4^2 \\ x_4 \\ -\dfrac{2Mx_1x_2x_4}{Mx_1^2 + J} - \dfrac{gx_1\cos x_3}{Mx_1^2 + J} - \dfrac{kx_3}{Mx_1^2 + J} \end{bmatrix},$$

$$g(x) = \begin{bmatrix} 0 \\ (1/M) \\ 0 \\ 0 \end{bmatrix}.$$

This system is easily linearized by the assumptions $\cos(x_i) \approx 1$, $\sin(x_i) \approx x_i$, and that any product of states (i.e., $x_1 x_4^2$) is very small or approximately zero.

https://doi.org/10.1017/S0263574707003797 Published online by Cambridge University Press

4. Controller Design

The grey theory used in ref. [24] to optimize the parameters of a PID controller for a robotic manipulator attached to a compliant base (one of SAMS types). Such a system is known as the macro–micro system, characterized by the number of control actuators being less than the number of state variables. However, the methodology requires a limited known data and needs to investigate the sensitivity of the control parameters, and then to predict the PID controller parameters. Therefore, a different approach will be proposed for stabilization of the equilibrium point of the system in this section: a state feedback controller [linear quadratic regulator (LQR)] plus a supervisory controller that will take control action in extreme situations for such a new pneumatic cart-seesaw system.

4.1. State feedback controller

Suppose that the realization of an equilibrium-to-equilibrium transfer maneuver of the sliding block is required in a finite time interval $[t_i, t_f]$. This is achieved by introducing a controlled displacement from given initial equilibrium positions, $(r(t_i), \theta(t_i))$, toward a second equilibrium position, $(r(t_f), \theta(t_f))$.

To ensure notational and analytical simplicity in linear system analysis and design, the linear system equations are often transferred such that the nominal (equilibrium) point is the origin of the state-space. The same action can be performed for nonlinear systems about a specific equilibrium point. Assume that the nominal (equilibrium) point of interest is x^*. The second equation in Eq. (4) yields the following implicit differential equation for the required nominal angular displacement, $\theta^*(t)$, in terms of the nominal longitudinal displacement, $r^*(t)$.

$$(Mr^*(t)^2 + J)\ddot{\theta}^*(t) + 2Mr^*(t)\dot{r}^*(t)\dot{\theta}^*(t) + Mgr^*(t)\cos\theta^*(t) + k\theta^*(t) = 0. \tag{6}$$

Then, by introducing a new variable

$$x_{1,\delta} = r - r^*, \quad x_{2,\delta} = \dot{r} - \dot{r}^*, \quad x_{3,\delta} = \theta - \theta^*, \quad x_{4,\delta} = \dot{\theta} - \dot{\theta}^*, \quad u_\delta = \tau - \tau^*.$$

The linearization of the system around the nominal trajectory $(r^*, \dot{r}^*, \theta^*, \dot{\theta}^*, \tau^*)$ is of the form

$$\dot{x}_\delta = Ax_\delta + Bu_\delta + \varepsilon h(x_\delta, u_\delta) \tag{7}$$

where $x_\delta = [x_{1,\delta}\ \ x_{2,\delta}\ \ x_{3,\delta}\ \ x_{4,\delta}]^T$, $A = (\frac{\partial f(x,\tau)}{\partial x})_{(x=0,\tau=0)}$, $B = (\frac{\partial f(x,\tau)}{\partial \tau})_{(x=0,\tau=0)}$, and $h \cong f(x,\tau) - Ax_\delta - Bu_\delta$. $\varepsilon \in [0, 1]$ is a scalar parameter.

Significantly, for $\varepsilon = 0$, the nonlinear system in Eq. (5) becomes linear, while for $\varepsilon = 1$, the linearized system in Eq. (7) corresponds to the original system. The control gain is easily obtained by assuming that $\varepsilon = 0$.

The following well-known approach is employed for a continuous linear quadratic regulator (LQR). Let the constant matrices Q and R be nonnegative and positive-definite, respectively. Define the performance index as

$$J(x_\delta, u_\delta) = \int_0^\infty \left(x_\delta^T Q x_\delta + u_\delta^T R u_\delta\right) dt \tag{8}$$

and the minimization problem as the task of finding an optimal control $u_\delta^*(\bullet)$, which minimizes J. To ensure the solvability of the problem, the pair (A, B) is required to be stabilizable. Therefore, the optimal control at time t is uniquely given by the control law

$$u_\delta^*(t) = -R^{-1}B^T K x_\delta(t) \tag{9}$$

where matrix K denotes the solution to the algebraic matrix Riccati equation (AMRE)

$$A^T K + KA - KBR^{-1}B^T K + Q = 0. \tag{10}$$

Hence, this investigation develops a linear state feedback controller for the stabilization of the linearized system, with the form

$$u_\delta = -k^T x_\delta = -k_1 x_{1,\delta} - k_2 x_{2,\delta} - k_3 x_{3,\delta} - k_4 x_{4,\delta} \tag{11}$$

with feedback gains $\{k_1, k_2, k_3, k_4\}$ selected so that the characteristic polynomial of the closed-loop system matrix, computed as $d(\lambda) = \det[\lambda \mathbf{I} - A + Bk^T]$, exhibits constant coefficients that coincide with those of a Hurwitz polynomial of the form $d(\lambda) = \lambda^4 + \gamma_4\lambda^3 + \gamma_3\lambda^2 + \gamma_2\lambda + \gamma_1$, whose roots are strictly in the left-half complex plane. Therefore, the main control action based on LQR is the PD controller.

However, for nonzero values of ε, Eq. (7) represents a nonlinear problem whose solution is typically difficult to obtain. Some near-optimum control designs have been developed to resolve this difficulty.[25] Nevertheless, the derivation procedure shown in those studies are laborious and time-consuming, particularly for a process with a nonlinear system. Hence, to avoid tedious and time-consuming tasks, the proposed system incorporates a supervisory controller.

4.2. Design of the supervisory controller

This section lists the details of how to construct a supervisory controller for a nonlinear control system where the state feedback controller already exists, and proposes modifications to the supervisory control such that it gradually switches to the supervisory mode. More specifically, this investigation designs a controller whose main control action is u_δ, and with a closed-loop system that is globally stable in the sense that the state x is uniformly bounded, i.e., $|x(t)| \le M_{x_\delta}$, $\forall t > 0$, where M_{x_δ} denotes a constant given by the designer.

For this task, a supervisory controller u_s, which is nonzero only when the state x hits the boundary of the constraint set $\{x : |x| \le M_{x_\delta}\}$, we append the PD controller u_δ. Thus, the control law is

$$u = u_\delta + I^* u_s \tag{12}$$

where the indicator function $I^* = 1$ if $|x| \ge M_{x_\delta}$, and $I^* = 0$ if $|x| < M_{x_\delta}$. Therefore, the main control action remains the

https://doi.org/10.1017/S0263574707003797 Published online by Cambridge University Press

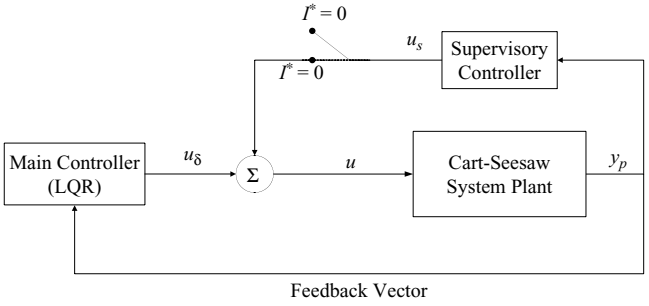

Fig. 7. Block diagram for the control structure.

PD control action. The value of u_s needs to be set such that $|x(t)| \leq M_{x_\delta}$ for all $t > 0$. If the main control action can perform successful control, then the supervisor just observes, and does not take any action. Otherwise, the supervisory controller begins operation. In this paper, the integral control action $u_s = k_I \int x_\delta \, dt$ is adopted for supervisory controller. Hence, the control structure with supervisory is the PID control form in this paper. Figure 7 displays the block diagram for the control structure.

As indicated above, the PD control is very effective if all the parameters of the system are known and no disturbance occurs. However, classical control theory states that PD control gives a nonzero steady-state error in the presence of constant disturbances. Consequently, the proposed system incorporates an integrator into the control loop—the supervisory control can be removed using the PID control law.

This seems to be because PID controllers, despite their simple structure, achieve acceptable performance for a wide range of industrial plants, and their usage (the tuning of their parameters) is well known among industrial operators.

5. Results and Discussions

5.1. Experiment implementation

Figure 8 shows the experimental setup. The seesaw can rotate only in a vertical plane with one degree of freedom,

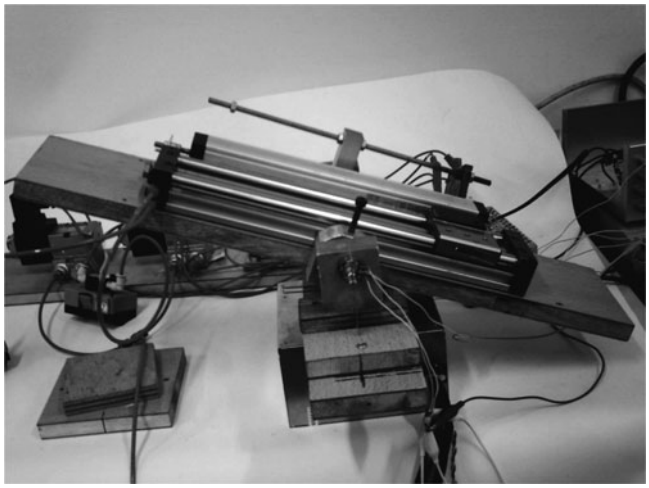

Fig. 8. Experimental apparatus for pneumatic cart-seesaw system.

Table I. Parameters of the system.

Parameters	Values
Moment of inertia of the beam, J	0.0904 (Nm)/s^2
Mass of the slide, M	0.368 kg
Torsion spring constant, k	0.1568 N/deg
Seesaw dimensions (length × width × height)	566 × 126 × 18 (mm)

and the cart slides along the seesaw by applying a force onto a pneumatic device. The aim of the experiment was to achieve a desired sliding mass position on the cart. Double solenoid proportional direction control valves were used to drive two double-acting pneumatic rodless cylinders. Table I presents the common properties of the test apparatus. The air supply was regulated to 6 bar (6 kgf/cm^2). The sampling time was 1 ms. The controller of the cart-seesaw system is composed of two NI DAQ boards (PCI-MIO-16E-4 and PCI-6174) with a host personal computer. The controller board with its real-time software interface permits rapid control prototyping in connection with LabVIEW, thus enabling a quick implementation of the proposed supervisory control approach on the basis of the real-time block model applied in LabVIEW.

5.2. Results

This section describes the experimental results of the proposed control scheme. The stabilization control for the equilibrium point is first presented. Figure 9 shows the performance of the proposed feedback controller based on approximate linearization around the equilibrium point. Figure 9(a) compares the cart's position in time response with and without supervisory control. This figure reveals that an LQR (the PD control form in this paper) had good transient tracking performance in this experiment. The feedback gains for LQR control were chosen as $k_1 = 6.73, k_2 = 2.23, k_3 = -0.38,$ and $k_4 = -0.16$ in the experiment. The values for control gains followed the LQR algorithm and attempted to achieve those values. However, Fig. 9(a) demonstrates that the performance significantly improved while the supervisory controller was being applied. The overshoot and steady-state error declined significantly. For such a case, the supervisory controller is selected as an integral control action, and its control gain is set to $k_I = 1$.

Figure 9(b) depicts the seesaw's angle response for the proposed control methodology. The tentative study [Fig. 9(b)] still demonstrates the performance of tracking with a large steady-state error under LQR control. However, a substantial improvement was achieved during tracking tasks by employing the proposed supervisory modification scheme. The supervisory controller increased the convergence rate and reduced the steady-state error. These results indicate that the use of a supervisory controller not only improves the tracking performance, but also eliminates control chattering. However, if the tracking controller cannot control the system well, then the supervisor takes control actions to prevent major problems. The tracking controller learns to collect the mistakes and regains control during this

https://doi.org/10.1017/S0263574707003797 Published online by Cambridge University Press

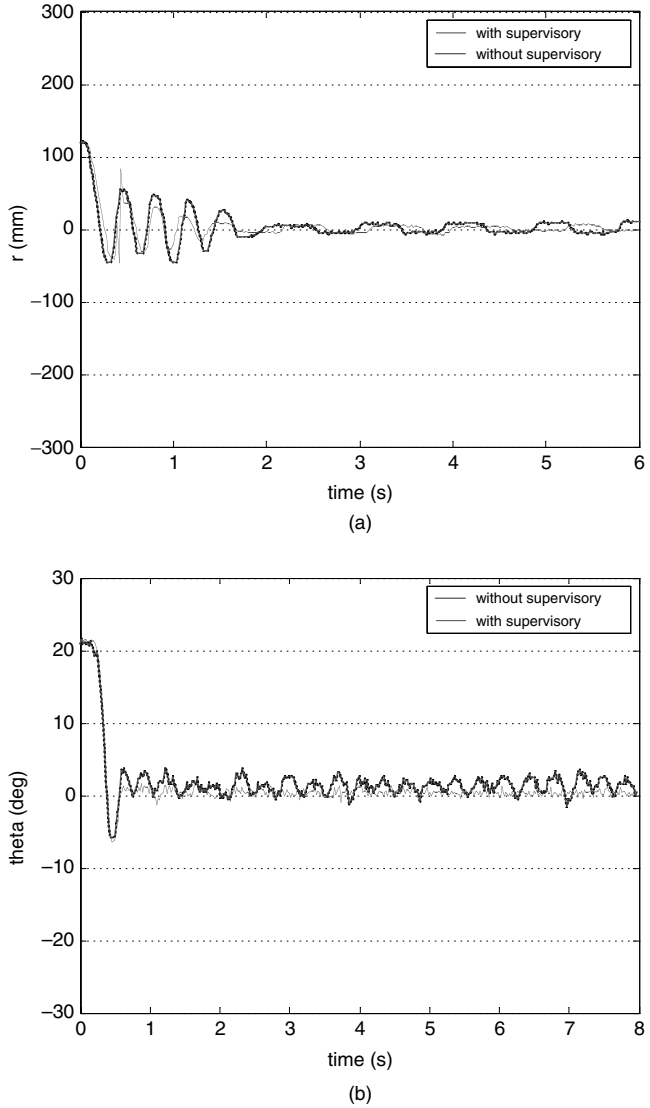

Fig. 9. Stabilization and control for equilibrium point. (a) Cart position. (b) Seesaw angle.

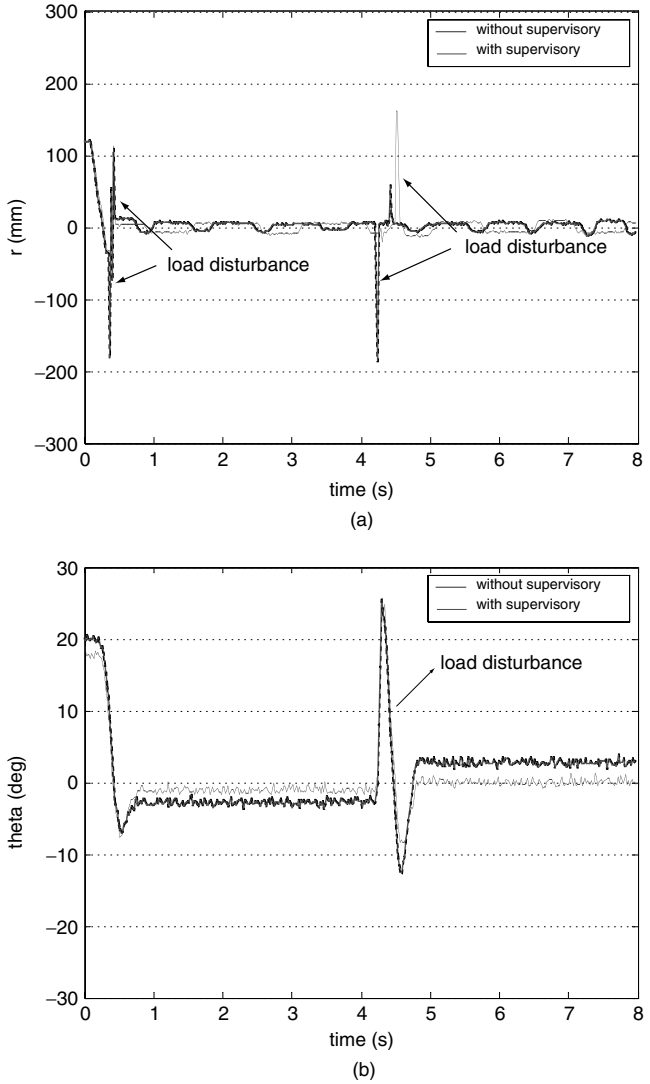

Fig. 10. Stabilization and control for equilibrium point with unexpected load disturbance. (a) Cart position. (b) Seesaw angle.

period. The supervisor becomes an observer again after the system returns to normal.

As demonstrated above, LQR is often appropriate for stabilization. However, LQR produces a residual error at the steady state due to gravity. This error can be eliminated using the PID control law (LQR with supervisory controller). For instance, the integral action has to be increased at the beginning of the transient response to shorten the rise time, and decreased when the system error is negative to reduce the overshoot.

Figure 10 plots the time response for cart position and seesaw angle with unexpected load disturbance, respectively. Figure 10(a) demonstrates that a pure LQR had a high transient tracking performance for cart position in the experiment. If the tracking controller can perform successful control, then the supervisory controller just observes and does not take any action. Furthermore, the tracking performance deteriorated when loading disturbance was applied to the seesaw angle under pure LQR control [Fig. 10(b)]. It also demonstrates that the seesaw angle θ performance improved significantly when the supervisory controller was applied. The steady-state error was reduced considerably. As before, the performance of the proposed controller was not significantly affected by the modification of system parameters, demonstrating the effectiveness of the controller in minimizing steady-state error in the time domain even when unexpected load disturbance occurs. The proposed LQR with supervisory control seems to have the required performance and robustness for such a case. Moreover, the proposed control methodology is a powerful and efficient way to cope with such a cart-seesaw system.

Figure 11 presents the performance for the LQR and LQR with supervisory under set point-to-point trajectory. The tracking performance for setting the point-to-point trajectory while applying the supervisory controller was found to be good. The proposed control modification scheme produced a substantial improvement in performance of the tracking tasks.

https://doi.org/10.1017/S0263574707003797 Published online by Cambridge University Press

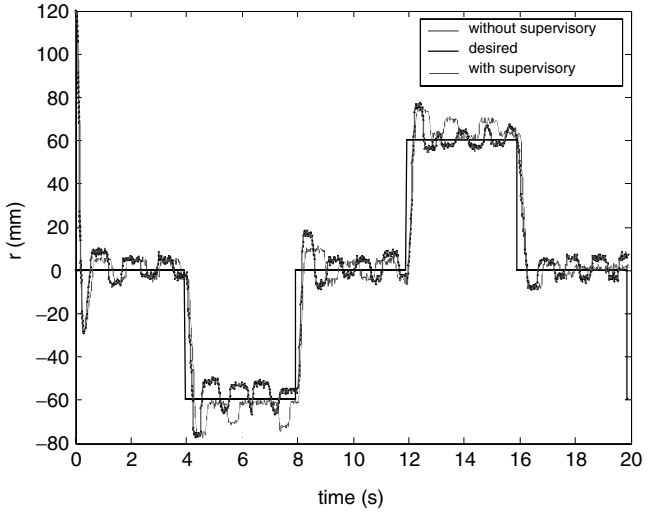

Fig. 11. Response for the cart position of the set point-to-point trajectory.

6. Conclusions

A new prototype of a cart-seesaw system has been developed in the Sensor and Control Laboratory of the Department of Mechanical Engineering at Ching Yun University. Modal analysis of the cart-seesaw, an interactive controller design, and controller evaluation is performed to demonstrate the utility of the environment as a research and education tool. This study also demonstrates a PC/LabVIEW-based interactive cart-seesaw control environment, which is valuable for upgrading the research and education process. This environment allows control system engineers and students to analyze, design, and visualize the performance of controllers in a complex mechanical system. A state feedback controller is adopted to stabilize the equilibrium point of the system. Moreover, this study incorporates a supervisory controller into the system to take control action in extreme situations. Experimental results indicate that utilizing the supervisory controller significantly enhances the performance. The overshoot and steady-state error are also reduced considerably. Thus, the test results demonstrate excellent control performance characteristics. The proposed system can be extensively applied in SAMS and pneumatic control systems in robotics control laboratories.

Acknowledgment

The authors would like to thank the National Science Council of the Republic of China, Taiwan, for financially supporting this research under Contract No. NSC 95-2221-E-231-010.

References

1. S. Uran and K. Jezernik, "Control of a Ball and Beam Like Mechanism," *Proceedings of the Advanced Metallization Conference* (2002) pp. 376–380.
2. G. Wang, Y. Tian and W. Hong, "Stabilization and Equilibrium Control of Super Articulated Ball and Beam System," *Proceedings of the 3rd World Congress on Intelligent Control and Automation* (2000) pp. 3290–3293.
3. S. Seto and J. Baillieul, "Control problems in super-articulated mechanical systems," *IEEE Trans. Autom. Control* **39**(12), 2442–2453 (1994).
4. A. M. Bloch, M. Reyhanoglu and N. H. McClamroch, "Control and stabilization of nonholonomic dynamic systems," *IEEE Trans. Autom. Control* **39**(12), 1746–1757 (1992).
5. G. Lafferriere and H. J. Sussmann, "Motion Planning for Controllable Systems Without Drift," *Proceedings of the IEEE International Conference on Robotics and Automation*, Sacramento, California (1991) pp. 1148–1153.
6. R. M. Murray and S. S. Sastry, "Nonholonomic motion planning: Steering using sinusoids," *IEEE Trans. Autom. Control* **38**, 700–716 (1993).
7. J. H. Choi and J. W. Grizzle, "Feedback control of an underactuated planar bipedal robot with impulsive foot action," *Robotica* **23**(5), 567–580 (2005).
8. M. Nikkhah, H. Ashrafiuon and F. Fahimi, "Robust control of underactuated bipeds using sliding modes," *Robotica* **25**(3), 367–374 (2007).
9. M. T. Hagan and C. D. Latino, "An Interdisciplinary Control Systems Laboratory," *Proceedings of the IEEE International Conference on Control Applications* 1996, pp. 403–408.
10. J. Hauser, S. Sastry and P. Kokotovic, "Nonlinear control via approximate input-output linearization: The ball and beam example," *IEEE Trans. Autom. Control* **37**(3), 392–398 (1992).
11. J. Huang and C.-F. Lin, "Robust Nonlinear Control of the Ball and Beam System," *Proceedings of the American Control Conference* (1995) pp. 306–310.
12. A. T. Simmons and J.-Y. Hung, "Hybrid Control of System With Poorly Defined Relative Degree: The Ball-on-Beam Example," *Proceedings of the 30th Annual Conference of the IEEE Industrial Electronics Society* (2004) pp. 2436–2440.
13. H. K. Lam, F. H. F. Leung and P. K. S. Tam, "Design of a Fuzzy Controller for Stabilizing a Ball-and-Beam System," *Proceedings of the IECON* (1999) pp. 520–524.
14. P. H. Eaton, D. V. Prokhorov and D. C. Wunsch II, "Neurocontroller alternatives for "fuzzy" ball-and-beam systems with nonuniform nonlinear friction," *IEEE Trans. Neural Netw.* **11**(2), 423–435 (2000).
15. X. Fan, N. Zhang and S. Teng, "Trajectory planning and tracking of ball and plate system using hierarchical fuzzy control scheme," *Fuzzy Sets Syst.* **144**, 297–312 (2003).
16. E. Richer and Y. Hurmuzlu, "A high performance pneumatic force actuator system: Part I—Nonlinear mathematical model," *Trans. ASME J. Dynam. Syst. Meas. Control* **122**, 416–425 (2000).
17. J. E. Bobrow and F. Jabbari, "Adaptive pneumatic force actuation and position control," *Trans. ASME J. Dynam. Syst. Meas. Control* **113**, 267–272 (1991).
18. B. W. McDonell and J. E. Bobrow, "Adaptive tracking control of an air powered robot actuator," *Trans. ASME J. Dynam. Syst. Meas. Control* **115**, 427–433 (1993).
19. P. K. Arun, J. K. Mishra and M. G. Radke, "Reduced order sliding mode control for pneumatic actuator," *IEEE Trans. Control Syst. Technol.* **2**(3), 271–276 (1994).
20. S. R. Pandian, Y. Hayakawa, Y. Kanazawa, Y. Kamoyama and S. Kawamura, "Practical design of a sliding moth controller for pneumatic actuators," *Trans. ASME J. Dynam. Syst. Meas. Control* **119**, 666 (1997).
21. E. Richer and Y. Hurmuzlu, "A high performance pneumatic force actuator system: Part I – Nonlinear Mathematical Model," *Trans. of the ASME Journal of Dynamic Systems, Measurement, and Control* **122**, 416–425 (2000).
22. E. Richer and Y. Hurmuzlu, "A high performance pneumatic force actuator system: Part II—Nonlinear controller design," *Trans. ASME J. Dynam. Syst. Meas. Control* **122**, 426–434 (2000).
23. D. McCloy and H. R. Martin, *Control of Fluid Power* (Ellis Horwood, New York, 1980).
24. J. Lin and Z.-Z. Huang, "A novel PID control parameters tuning approach for robot manipulators mounted on oscillatory bases," *Robotica* **25**(4), 467–477 (2007).
25. M. Jamshidi, *Large-Scale Systems: Modeling, Control, and Fuzzy Logic* (Prentice Hall, Englewood cliffs, NJ, 1996).

Appendix

Kinetic energy of the cart:

$$\begin{aligned} K_1 &= \frac{1}{2}M(\dot{x}^2 + \dot{y}^2) \\ &= \frac{1}{2}M[(\dot{r}c\theta - r\dot{\theta}s\theta)^2 + (\dot{r}s\theta + r\dot{\theta}c\theta)^2] \\ &= \frac{1}{2}M(\dot{r}^2 + r^2\dot{\theta}^2). \end{aligned}$$

Kinetic energy of the seesaw:

$$K_2 = \frac{1}{2}J\dot{\theta}^2.$$

Potential energy of the ball:

$$V_1 = Mgr\sin\theta.$$

Potential energy of the spring:

$$V_2 = \frac{1}{2}k\theta^2.$$

Total kinetic energy:

$$K = K_1 + K_2.$$

Total potential energy:

$$V = V_1 + V_2.$$

Now, we derive the equations of motion by using Lagrange's formulation:

$$\frac{d}{dt}\frac{\partial L}{\partial \dot{q}_i} - \frac{\partial L}{\partial q_i} = \tau$$

where $L = K - V$ and $q_i = [r \quad \theta]^T$.

Therefore, the dynamic equation can be shown in the following form:

$$M\ddot{r} + Mg\sin\theta - Mr\dot{\theta}^2 = \tau$$

$$(Mr^2 + J)\ddot{\theta} + 2Mr\dot{r}\dot{\theta} + Mgr\cos\theta + k\theta = 0.$$

https://doi.org/10.1017/S0263574707003797 Published online by Cambridge University Press